Inelastic scattering of ^{18}O and ^{17}O ions from medium-weight nuclei

H. Essel, K. E. Rehm, H. Bohn, H. J. Körner, and H. Spieler*
Physik Department, Technische Universität München, D-8046 Garching, West Germany
(Received 27 November 1978)

Inelastic scattering of ^{18}O and ^{17}O ions from various target nuclei in the mass range $A = 48$–92 has been investigated at incident energies between 54 and 69 MeV. Angular distributions for the excitation of the first excited states in the target nuclei are well reproduced by conventional distorted-wave Born approximation calculations with $B(E2)$ values from the literature, and equal charge and mass deformation lengths. The measured angular distributions for the excitation of the first excited state in ^{18}O are, however, shifted to forward angles by 2°–5° (c.m.) with respect to the theoretical calculations. This shift is more pronounced for target nuclei near closed neutron shells. Furthermore, ^{18}O and ^{17}O induced one and two neutron transfer reactions on some of these nuclei have been measured. The systematics observed in our inelastic scattering and transfer studies suggest that two step processes including neutron transfer channels as intermediate steps are responsible for these observed shifts.

[NUCLEAR REACTIONS $^{48}Ti(^{18}O,^{18}O)$, $E=45$ MeV; $^{52}Cr(^{18}O,^{18}O)$, $E=56$ MeV; $^{54}Fe(^{18}O,^{18}O)$, $E=60$ MeV; $^{72}Ge(^{18}O,^{18}O)$, $E=68.6$ MeV; $^{91}Zr(^{18}O,^{18}O)$, $E=68.6$ MeV; $^{92}Zr(^{18}O,^{18}O)$, $E=68.5$ MeV; measured $\sigma(\theta)$ for g.s. and first 2^+ states in ^{18}O, ^{48}Ti, ^{52}Cr, ^{54}Fe, ^{72}Ge, ^{92}Zr and for first $1/2^+$ state in ^{91}Zr. $^{54}Fe(^{17}O,^{17}O)$, $E=59.1$ MeV; $^{60}Ni(^{17}O,^{17}O)$, $E=62.1$ MeV; measured $\sigma(\theta)$ for g.s. and first 2^+ states in ^{54}Fe, ^{60}Ni and for first $1/2^+$ state in ^{17}O. $^{72}Ge(^{18}O,^{18}O)$, $E=30$–48 MeV, $\theta_{lab}=175°$; measured $\sigma(E)$ for the first 2^+ states in ^{72}Ge and ^{18}O. $^{54}Fe(^{18}O,^{17}O)$, $E=56$ MeV; $^{120}Sn(^{18}O,^{17}O)$, $E=72$ MeV; measured $\sigma(\theta)$ for low lying states. $^{54}Fe(^{17}O,^{16}O)$, $E=59.1$ MeV; $^{60}Ni(^{17}O,^{16}O)$, $E=62.1$ MeV; measured $\sigma(\theta)$ for low lying states. Optical model, DWBA, deformation parameters. Enriched targets.]

I. INTRODUCTION

The Coulomb-nuclear interference in the inelastic scattering of heavy ions at energies above the Coulomb barrier is usually thought to be a well understood process. The oscillations in the angular distributions for transitions to low lying collective 2^+ and 3^- states in medium-weight nuclei, which are out of phase with the corresponding oscillations in the elastic scattering angular distribution σ/σ_R, are well described by distorted-wave Born approximation (DWBA) calculations, if Coulomb excitation is properly taken into account.[1-10] The oscillations in the angular distributions can be understood in the framework of different semiclassical models.[11] There are anomalies, however, observed in the angular distributions and excitation functions for the $0^+ \rightarrow 2^+$ transitions in ^{12}C (Refs. 6 and 7), ^{18}O (Refs. 5 and 12), ^{20}Ne (Refs. 9 and 10), ^{22}Ne (Ref. 4), and ^{24}Mg (Ref. 8). In general, the measured angular distributions show a shift $\Delta\theta$ varying between 2° and 5° (c.m.) towards forward angles with respect to the DWBA calculations. Several explanations have been suggested in order to explain this behavior:

(i) An unusually large reorientation effect causes a shift of the whole angular distribution pattern towards forward angles as shown in a semiclassical calculation by Broglia[13] for the case of ^{18}O. Quantitative coupled channels (CC) calculations[12] have shown, however, that the quadrupole moment of the 2^+ state in ^{18}O (Ref. 14) is much too small to produce a sizable shift of the angular distribution. Recently, experiments have been performed for the inelastic excitation of the 2^+ state in ^{20}Ne (Refs. 9 and 10). For the reaction $^{20}Ne + ^{40}Ca$ the influence of the quadrupole moment in CC calculations cannot account for the total shift of about 5° observed[9] in the angular distributions. A similar conclusion must be drawn from the analysis of excitation functions.[9] For the system $^{20}Ne + ^{208}Pb$, however, the CC calculations seem to be sensitive if reasonable values for the quadrupole moment are chosen.[10]

(ii) Microscopic calculations with folded potentials have been performed recently[15] in order to explain the anomaly observed for ^{18}O (2^+). These microscopic form factors have a larger radial width than the usual form factor calculated

within the framework of the collective model. Modified form factors can reproduce the observed shift of the angular distribution, as already shown in Ref. 5. However, excitation functions measured at backward angles[5] are not explained (see also Sec. V E).

(iii) A coupled reaction channels (CRC) calculation[16] for the system $^{18}O + ^{60}Ni$ has shown that intermediate routes such as $(^{18}O, ^{17}O) \otimes [^{17}O, ^{18}O(2^+)]$ have to be taken into account. No CRC calculations for other systems have been performed to our knowledge. The success of this calculation suggest that the *ad hoc* change of the phase of the complex form factor,[5,17] which so far is the only way to describe angular distributions and excitation functions for the 2^+ state in ^{18}O, just simulates coupled channels effects.

In order to investigate whether there is a systematic behavior in the shift $\Delta\theta$ of the angular distribution for the excitation of the 2^+ state in ^{18}O we have measured inelastic scattering of ^{18}O ions from medium-weight nuclei with masses between $A = 48$ and $A = 92$. For some of the systems the cross sections of the $(^{18}O, ^{17}O)$ and $(^{18}O, ^{16}O)$ reactions were also determined. In addition, we have measured elastic and inelastic scattering of ^{17}O in order to study the influence of transfer channels on the excitation of the $\frac{1}{2}^+$, 0.871 MeV state in ^{17}O.

II. EXPERIMENTAL DETAILS

The experiments were performed at the Munich MP tandem accelerator, with ^{17}O and ^{18}O beams extracted from a Penning source. A detailed description of the experimental setup used for the measurement of angular distributions and excitation functions is given in Ref. 5. The target-projectile combinations investigated in this work are summarized in Table I. The energy resolution in the data presented here is about 250 keV, mainly due to kinematic broadening and energy straggling in the targets. Thus transitions to the first excited states could be separated from the elastic peak for scattering angles larger than $\theta_{lab} \approx 20°$. The ^{52}Cr target showed deterioration effects at beam currents of >100 nA resulting in a somewhat poorer energy resolution. Owing to the use of single detectors in our experiments, ^{17}O and ^{16}O ions from the one and two neutron transfer channels $(^{18}O, ^{17}O)$ and $(^{18}O, ^{16}O)$ could not be separated from inelastically scattered ^{18}O ions of the same energy. As shown in Ref. 5, transfer reactions influence the magnitude of the cross section at larger angles to some extent; the oscillatory structure of the angular distribution is, however, not affected. Because of the positive Q values, angular distributions for transfer reactions to low lying states could also be measured with single detectors for cases $^{54}Fe(^{18}O, ^{17}O)^{55}Fe$, $^{54}Fe(^{17}O, ^{16}O)^{55}Fe$, and $^{60}Ni(^{17}O, ^{16}O)^{61}Ni$. For the $^{120}Sn(^{18}O, ^{17}O)^{121}Sn$ reaction a ΔE-E time of flight technique had to be applied.[18]

TABLE I. Target-projectile combinations investigated in the present work.

Target nucleus	Projectile	E_{lab} (MeV)	Measured quantities
^{48}Ti	^{18}O	54	Angular distributions
^{52}Cr	^{18}O	56	Angular distributions
^{54}Fe	^{18}O	60	Angular distributions
^{54}Fe	^{17}O	59.1	Angular distributions
^{60}Ni	^{17}O	62.1	Angular distributions
^{72}Ge	^{18}O	68.6	Angular distributions
^{72}Ge	^{18}O	30–48	Excitation function at $\theta_{lab} = 175°$
^{91}Zr	^{18}O	68.6	Angular distributions
^{92}Zr	^{18}O	68.5	Angular distributions

III. THEORETICAL ANALYSIS

The experimental data were analyzed with the optical model code ABACUS[19] for elastic scattering and the DWBA code DWIN[20] for the inelastic channels. A six parameter Woods-Saxon potential was

TABLE II. Optical potential parameters obtained from a least squares fit to the elastic scattering angular distributions. The parameters are defined in Sec. III.

Reaction	E_{lab} (MeV)	V (MeV)	r_0 (fm)	a (fm)	W (MeV)	r_0' (fm)	a' (fm)
$^{48}Ti + ^{18}O$	54	17.5	1.33	0.57	5.7	1.37	0.56
$^{52}Cr + ^{18}O$	56	15.0	1.33	0.56	10.9	1.30	0.59
$^{54}Fe + ^{18}O$	60	31.9	1.28	0.51	12.8	1.28	0.57
$^{72}Ge + ^{18}O$	68.6	97.9	1.19	0.60	41.4	1.13	0.65
$^{91}Zr + ^{18}O$	68.6	14.6	1.36	0.52	6.9	1.39	0.51
$^{92}Zr + ^{18}O$	68.5	20.9	1.33	0.53	10.8	1.35	0.51
$^{54}Fe + ^{17}O$	59.1	34.1	1.29	0.51	6.1	1.32	0.53
$^{60}Ni + ^{17}O$	62.1	13.4	1.35	0.59	8.8	1.37	0.40

used in the optical model search:

$$V = V_c(r) - Vf(r) - iWg(r),$$

where

$$V_c(r) = \frac{Z_1 Z_2 e^2}{r}, \quad r > R_c,$$

$$V_c(r) = \frac{Z_1 Z_2 e^2}{2R_c}\left(3 - \frac{r^2}{R_c^2}\right), \quad r \leq R_c, \quad R_c = r_{0c} A_2^{1/3},$$

$$f(r) = \left[1 + \exp\frac{r - R_0}{a}\right]^{-1}, \quad R_0 = r_0(A_1^{1/3} + A_2^{1/3}),$$

$$g(r) = \left[1 + \exp\left(\frac{r - R_0'}{a'}\right)\right]^{-1}, \quad R_0' = r_0'(A_1^{1/3} + A_2^{1/3}).$$

A_1, Z_1 and A_2, Z_2 are the mass and charge of projectile and target, respectively.

A form factor $F_2(r)$ consisting of a Coulomb and a nuclear part was used to describe the inelastic excitation of the 2^+ states:

$$F_2(r) = F_2^c(r) + F_2^N(r).$$

The Coulomb part is given by

$$F_2^c(r) = \frac{4\pi Z_1 e}{5}[B(E2;\uparrow)]^{1/2} \times \frac{1}{r^3}, \quad \text{for } r > R_c,$$

$$F_2^c(r) = \frac{4\pi Z_1 e}{5}[B(E2;\uparrow)]^{1/2} \times \frac{r^2}{R_c^5}, \quad \text{for } r \leq R_c,$$

with $R_c = r_{0c} A_2^{1/3}$ and $r_{0c} = 1.25$ fm.

The nuclear part of the form factor was calculated within the framework of the collective model:

$$F_2^N(r) = \left(\beta_2^N R_2 V \frac{df(r)}{dr} + i\beta_2^N R_2 W \frac{dg(r)}{dr}\right).$$

Two parameters, $B(E2;\uparrow)$ and $\beta_2^N R_2$, enter the calculation. The $B(E2;\uparrow)$ values which determine the absolute overall cross section were taken from the literature. The nuclear deformation length $\beta_2^N R_2$ which influences the amplitude of the oscillations in the angular distributions was assumed to be equal to the charge deformation length $\beta_2^c R_c$.

The one neutron transfer DWBA calculations were performed with the exact finite range program **PTOLEMY**.[21] The bound state wave functions were computed using the conventional separation energy prescription. The binding potential has the form

$$U(r) = -V_0 f(r) + \left(\frac{\lambda}{45.2}\right)\left(\frac{\vec{L}\cdot\vec{S}}{r}\right)V_0 \frac{df(r)}{dr}.$$

The spin-orbit strength parameter λ was chosen to be either 0 or 25. Both calculations resulted in angular distributions with identical shapes but slightly changed absolute magnitude. In all cal-

TABLE III. Deformation lengths and $B(E2)$ values used in the DWBA calculations.

Target nucleus	J^π ($\hbar$)	E^* (MeV)	$B(E2;\uparrow)$ (e^2b^2)	δ_c (fm)	δ_N (fm) (p,p')	(d,d')	(t,t')	$(^3\mathrm{He},^3\mathrm{He}')$	(α,α')	$(^{13}\mathrm{C},^{13}\mathrm{C}')$	$(^{16}\mathrm{O},^{16}\mathrm{O}')$	$(^{17}\mathrm{O},^{17}\mathrm{O}')$	$(^{18}\mathrm{O},^{18}\mathrm{O}')$
^{48}Ti	2^+	0.983	0.071	1.12[a]	1.0[e]	0.87[m]	...	0.84[q]	1.17[s]	...	...	...	1.12[z]
^{52}Cr	2^+	1.434	0.067	0.97[a]	0.77[f]	0.75[m]	...	0.60[q]	0.62[t]	...	...	...	0.97[z]
^{54}Fe	2^+	1.408	0.052	0.78[b]	0.59[g]	0.67[m]	...	...	0.50[t]	...	0.72[x]	...	0.78[z]
^{60}Ni	2^+	1.333	0.091	0.92[a]	1.20[h]	0.99[n]	...	1.3[r]	1.16[u]	1.1[w]	0.92[y]	0.92[z]	0.74[y]
^{72}Ge	2^+	0.834	0.155	0.99[z]	1.13[i]	...	...	...	...	...	...	...	0.99[z]
^{91}Zr	$\frac{1}{2}^+$	1.205	0.007	0.16[c]	0.96[k]	...	...	...	...	...	...	...	0.73[z]
^{92}Zr	2^+	0.934	0.079	0.52[d]	0.66[l]	0.51[o]	0.62[p]	0.7[r]	0.64[v]	...	...	...	0.52[z]
^{18}O	2^+	1.982	0.0039	1.0[a]	...	...	...	...	...	...	...	...	1.0[z]

[a] Reference 26. [e] Reference 30. [i] Reference 34. [n] Reference 38. [r] Reference 42. [v] Reference 46. [z] This work.
[b] Reference 27. [f] Reference 31. [k] Reference 35. [o] Reference 39. [s] Reference 43. [w] Reference 47.
[c] Reference 28. [g] Reference 32. [l] Reference 36. [p] Reference 40. [t] Reference 44. [x] Reference 48.
[d] Reference 29. [h] Reference 33. [m] Reference 37. [q] Reference 41. [u] Reference 45. [y] Reference 5.

TABLE IV. Spectroscopic factors used in the DWBA calculations. The bound state parameters were $r_0 = 1.20$ fm and $a = 0.65$ fm for ^{17}O and ^{18}O, and $r_0 = 1.25$ fm and $a = 0.65$ fm for ^{55}Fe, ^{61}Ni and ^{121}Sn. The spin-orbit strength parameter used was $\lambda = 25$.

Bound state	E^* (MeV)	J^π ($\hbar$)	c^2s		E_x (MeV)	J^π ($\hbar$)	c^2s	$(\sigma_{exp}/\sigma_{DWBA})_{max}$
$^{54}Fe+n$	0.0	$\frac{3}{2}^-$	0.46 [a]	$^{17}O+n$	0.0	$\frac{5}{2}^+$	1.31 [b]	1.61
	0.412	$\frac{1}{2}^-$	0.31 [a]	$^{17}O+n$	0.0	$\frac{5}{2}^+$	1.31	1.86
$^{120}Sn+n$	0.0	$\frac{3}{2}^+$	0.43 [c]	$^{17}O+n$	0.0	$\frac{5}{2}^+$	1.31	...
	0.008	$\frac{11}{2}^-$	0.21 [c]	$^{17}O+n$	0.0	$\frac{5}{2}^+$	1.31	1.17
	0.058	$\frac{1}{2}^+$	0.39 [c]	$^{17}O+n$	0.0	$\frac{5}{2}^+$	1.31	...
	0.0	$\frac{3}{2}^+$	0.43 [c]	$^{17}O+n$	0.871	$\frac{1}{2}^+$	0.07 [b]	...
	0.008	$\frac{11}{2}^-$	0.21 [c]	$^{17}O+n$	0.871	$\frac{1}{2}^+$	0.07	...
	0.058	$\frac{1}{2}^+$	0.39 [c]	$^{17}O+n$	0.871	$\frac{1}{2}^+$	0.07	3.0
	0.934	$\frac{7}{2}^+$	0.19 [c]	$^{17}O+n$	0.0	$\frac{5}{2}^+$	1.31	...
$^{54}Fe+n$	0.0	$\frac{3}{2}^-$	0.46 [a]	$^{16}O+n$	0.0	$\frac{5}{2}^+$	1 [d]	1.02
	0.412	$\frac{1}{2}^-$	0.31 [a]	$^{16}O+n$	0.0	$\frac{5}{2}^+$	1	1.08
	0.931	$\frac{5}{2}^-$	0.352 [a]	$^{16}O+n$	0.0	$\frac{5}{2}^+$	1	1.35
$^{60}Ni+n$	0.0	$\frac{3}{2}^-$	0.395 [e]	$^{16}O+n$	0.0	$\frac{5}{2}^+$	1	...
	0.067	$\frac{5}{2}^-$	0.533 [e]	$^{16}O+n$	0.0	$\frac{5}{2}^+$	1	0.62
	0.283	$\frac{1}{2}^-$	0.610 [e]	$^{16}O+n$	0.0	$\frac{5}{2}^+$	1	...
	1.133	$\frac{5}{2}^-$	0.06 [e]	$^{16}O+n$	0.0	$\frac{5}{2}^+$	1	...
	1.186	$\frac{3}{2}^-$	0.063 [e]	$^{16}O+n$	0.0	$\frac{5}{2}^+$	1	1.15
	2.114	$\frac{9}{2}^+$	0.78 [e]	$^{16}O+n$	0.0	$\frac{5}{2}^+$	1	0.72

[a] Reference 55.
[b] Reference 56.
[c] Reference 57.
[d] Reference 58.
[e] Reference 59.

culations the effective interaction included the core – Coulomb correction factor as discussed by DeVries *et al.*[22] The parameters used in the calculations are summarized in Tables II–IV.

IV. EXPERIMENTAL RESULTS

The experimental results of the present investigation are shown in Figs. 1–9 for elastic and inelastic scattering, and in Figs. 10 and 11 for the transfer channels. The solid curves are the result of optical model (elastic) and DWBA calculations (inelastic scattering and transfer reactions) as described in Sec. III. The following general features are observed in the data:

(a) The angular distributions for the excitation of both the target and the projectile show an oscillatory behavior which is more pronounced for the projectile excitation.

(b) The last minimum in the angular distribution for the target excitation is slightly shifted towards larger angles if compared to the Fresnel maximum in the elastic scattering angular distribution due to the negative Q value for the inelastic scattering.

(c) Contrary to the target excitation, the last minimum in the angular distribution for the excitation of the 2^+ state in ^{18}O is not shifted towards backward angles; in general it coincides with the Fresnel maximum. This behavior will be discussed in more detail in Sec. V B.

(d) The excitation function for the 2^+ state in ^{72}Ge is dominated by the Coulomb form factor and does not show the characteristic pattern observed for $2^+ \rightarrow 0^+$ transitions in ^{60}Ni and ^{92}Mo (see Ref. 5). However, the projectile excitation function is similar to those described in Ref. 5.

(e) The angular distributions for the one neutron transfer channels (^{18}O, ^{17}O) and (^{17}O, ^{16}O) are bell

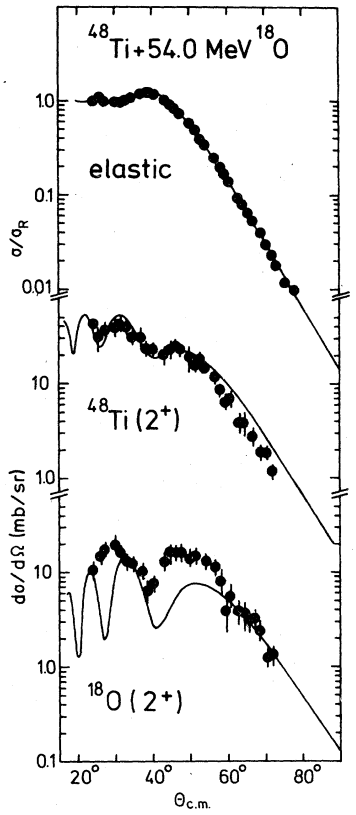

FIG. 1. Angular distributions for elastic scattering and inelastic excitation of the lowest 2^+ states in ^{48}Ti and ^{18}O. The solid lines are optical model (elastic) and DWBA calculations (inelastic) with parameters given in Tables II and III.

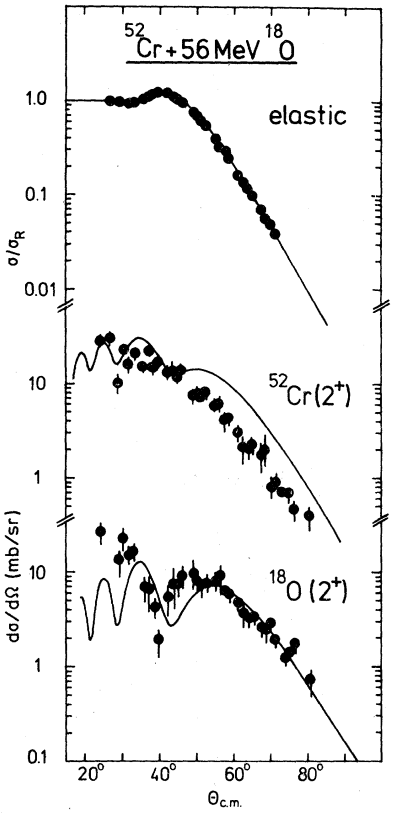

FIG. 2. Angular distributions for elastic scattering and inelastic excitation of the lowest 2^+ states in ^{52}Cr and ^{18}O. The solid lines are optical model (elastic) and DWBA calculations (inelastic) with parameters given in Tables II and III.

shaped with a somewhat increased cross section at forward angles.

V. DISCUSSION

A. Elastic scattering and target excitation

The parameters obtained from a least squares fit to the elastic scattering angular distributions are summarized in Table II. Potentials with six parameters were used in the analysis. It was verified that other potential families describe the elastic and inelastic scattering data with the same degree of accuracy; this finding agrees with the results obtained in Ref. 23. Using the optical potential parameters obtained from the analysis of elastic scattering and assuming equal charge and mass deformation lengths in the DWBA calculations, we have calculated the distributions shown as solid lines in Figs. 1–9. In general the agreement between the experimental data and the theoretical prediction is good. In this context two comments have to be made: (1) For the excitation of the 2^+ state in ^{72}Ge a $B(E2;\uparrow)$ value of 0.155 e^2b^2 had to be used in the calculations in order to reproduce the magnitude of the observed cross section. This value is about 30% smaller than the one calculated from the half-life of the 2^+ state, but is in good agreement with the result of an earlier (α, α') experiment analyzed by Temmer *et al.*[24] The reason for this discrepancy is not known. CC calculations with the program CHUCK[28] including the coupling to the first 2^+ states at 0.834 MeV and 1.464 MeV in ^{72}Ge reproduce the result of the DWBA calculation. (2) For the $\frac{5}{2}^+ \rightarrow \frac{1}{2}^+$ transition in ^{91}Zr the DWBA calculation underestimates the cross section by a factor of 3. For this single particle transition the assumption that the nuclear deformation length $\beta_2^N R$ can be calculated from the corresponding $B(E2;\uparrow)$ value is not justified. Therefore, $\beta_2^N R$ was treated as a free parameter in the DWBA calculation.

All deformation parameters used in the calcu-

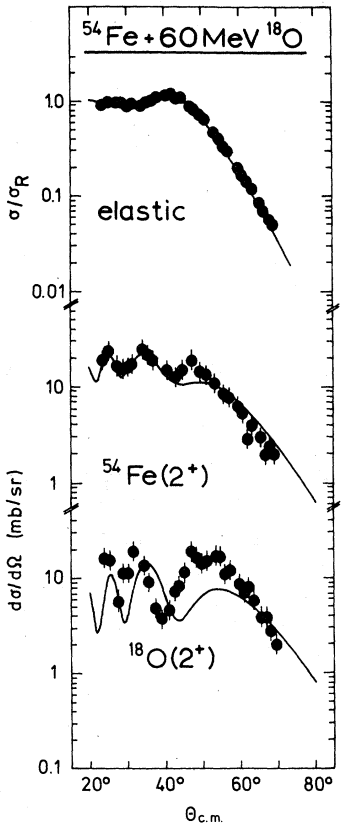

FIG. 3. Angular distributions for elastic scattering and inelastic excitation of the lowest 2^+ states in ^{54}Fe and ^{18}O. The solid lines are optical model (elastic) and DWBA calculations (inelastic) with parameters given in Tables II and III.

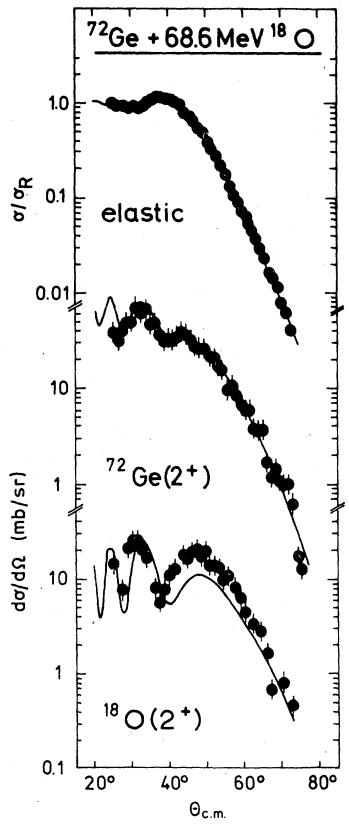

FIG. 4. Angular distributions for elastic scattering and inelastic excitation of the lowest 2^+ states in ^{72}Ge and ^{18}O. The solid lines are optical model (elastic) and DWBA calculations (inelastic) with parameters given in Tables II and III.

lations are summarized in Table III together with the corresponding values from other studies. In general the nuclear deformation lengths δ_N obtained from the analysis of reactions with different projectiles agree within 20% (see Table III).

B. The excitation of ^{18}O (2^+)

A comparison of the experimental angular distributions with the DBWA calculation for the excitation of the first excited 2^+ state in ^{18}O reveals two characteristic features (1) Usually the DWBA cross section at the last maximum preceding the exponential falloff in the angular distribution is too small by a factor of 2 (see Figs. 1–6). This effect is especially pronounced for the ^{54}Fe (Fig. 3), ^{91}Zr (Fig. 5), and ^{92}Zr (Fig. 6) targets. It should be noted that within this angular region nuclear excitation and transfer processes are expected to have the largest influence on the cross section. (2) The shift of the last minimum in the angular distribution with respect to the DWBA calculation is larger for the ^{54}Fe, ^{91}Zr, and ^{92}Zr targets than for the ^{48}Ti and ^{72}Ge targets. A similar behavior was observed in Ref. 5: The shift is larger for ^{92}Mo if compared to $^{58-64}Ni$ and ^{120}Sn.

It was verified that the position of the last minimum in the DWBA calculation does not depend on the optical model parameters chosen for the calculation as long as the elastic scattering angular distribution is reproduced. Figure 12 summarizes all the shifts of the angular distributions between the DWBA prediction and the data, $\Delta\theta = \theta_{DWBA} - \theta_{exp}$, which could be reliably extracted for different target nuclei. Figure 12(a) shows the shift for the last minimum of the angular distribution while Fig. 12(b) corresponds to the preceding maximum. The error bars given in Fig. 12 are the sum of the systematic angle uncertainty of the experimental setup and the error determined from the angular distributions using a least squares fitting routine. A systematic variation of

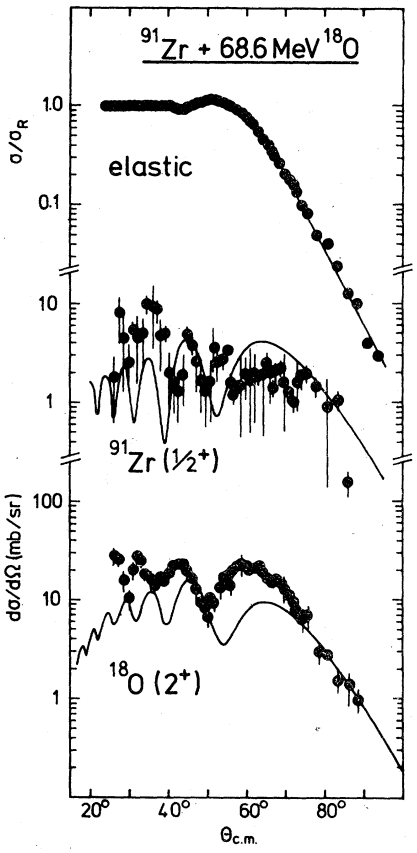

FIG. 5. Angular distributions for elastic scattering and inelastic excitation of the $\frac{1}{2}^+$ state at $E^*=1.205$ MeV in ^{91}Zr and the 2^+ state at 1.982 MeV in ^{18}O. The solid lines are optical model (elastic) and DWBA calculations (inelastic) with parameters given in Tables II and III.

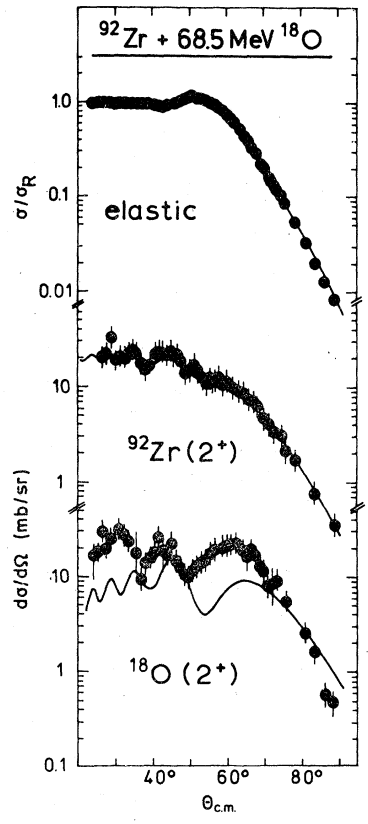

FIG. 6. Angular distributions for elastic scattering and inelastic excitation of the lowest 2^+ states in ^{92}Zr and ^{18}O. The solid lines are optical model (elastic) and DWBA calculations (inelastic) with parameters given in Tables II and III.

the shift as a function of the target nucleus is evident from Fig. 12. The largest shift is observed for nuclei near closed neutron shells, e.g., ^{52}Cr, ^{54}Fe, ^{91}Zr, ^{92}Zr, ^{92}Mo, while it is smaller for the other cases investigated: ^{48}Ti, ^{58,60,62,64}Ni, ^{72}Ge, ^{120}Sn. A similar dependence for the nuclei near closed proton shells is not observed. This strong variation of the shift in the inelastic scattering angular distribution cannot be understood if reorientation effects in the ^{18}O 2^+ state are responsible for the discrepancy. Since neutron binding energies are minimal for orbitals just outside closed shells, the radial form factors, which strongly influence the transfer cross sections, extend to larger radii in these cases. Therefore, the large shift for nuclei near closed neutron shells suggests that one and two neutron transfer reactions influence the excitation of the 2^+ state in ^{18}O.

C. The ^{54}Fe(^{18}O, ^{17}O)^{55}Fe and ^{120}Sn(^{18}O, ^{17}O)^{121}Sn transfer reactions

Calculations in the CRC formalism by Low[16] including the one neutron transfer reaction (^{18}O, ^{17}O) as an intermediate channel were successful in explaining the observed[5] shift for ^{18}O + ^{60}Ni. We have therefore investigated the reactions ^{54}Fe(^{18}O, ^{17}O)^{55}Fe and ^{120}Sn(^{18}O, ^{17}O)^{121}Sn to low lying states in ^{55}Fe and ^{121}Sn, respectively. These reactions are the two cases which show one of the largest difference in the shifts $\Delta\theta$ for the inelastic scattering angular distributions (see Fig. 12). The results are shown in Fig. 10. The solid curves are DWBA calculations described in Sec. III, with spectroscopic factors summarized in Table IV. Owing to the energy resolution of about 300 keV for the time of flight telescope, the individual transitions to the $\frac{3}{2}^+$, $\frac{11}{2}^-$, and $\frac{1}{2}^+$ states in ^{121}Sn could not be resolved. The angular distribution for the states near the 0.9 MeV ex-

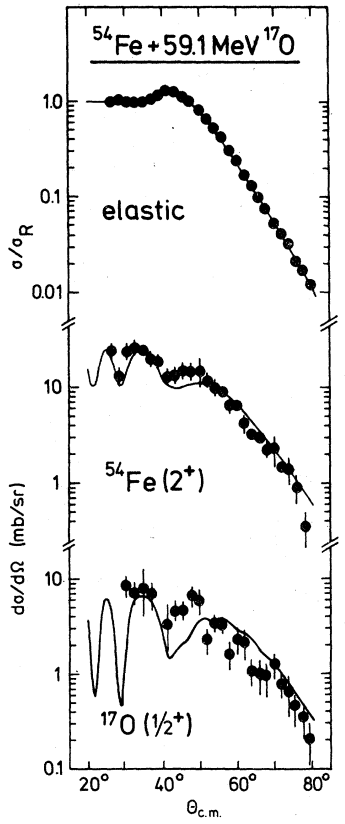

FIG. 7. Angular distributions for elastic scattering and inelastic excitation of the lowest 2^+ state in ^{54}Fe and the $\frac{1}{2}^+$ state at $E^*=0.871$ MeV in ^{17}O. The solid lines are optical model (elastic) and DWBA calculations (inelastic) with parameters given in Tables II and III. For the excitation of the $\frac{1}{2}^+$ state in ^{17}O a $B(E2)$ value of $B(E2;\uparrow) = 0.000\,21\ e^2b^2$ and a nuclear deformation length $\delta_N = 0.72$ fm was used.

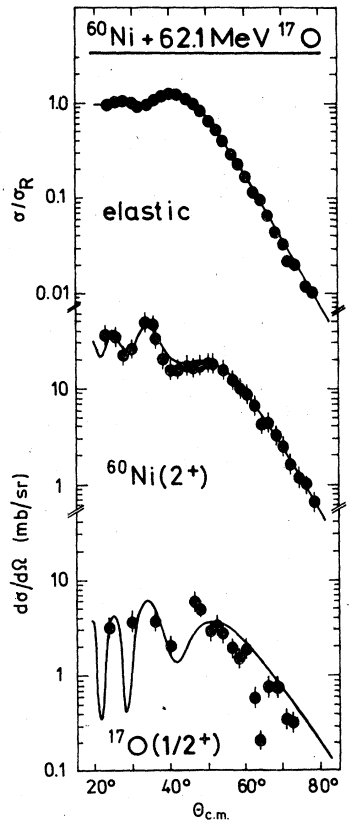

FIG. 8. Angular distributions for elastic scattering and inelastic excitation of the lowest 2^+ state in ^{60}Ni and the $\frac{1}{2}^+$ state at $E^*=0.871$ MeV in ^{17}O. The solid lines are optical model (elastic) and DWBA calculations (inelastic) with parameters given in Tables II and III. For the excitation of the $\frac{1}{2}^+$ state in ^{17}O a $B(E2)$ value of $B(E2;\uparrow) = 0.000\,21\ e^2b^2$ and a nuclear deformation length $\delta_N = 0.66$ fm was used.

citation includes the transitions to the $\frac{7}{2}^+$ state in ^{121}Sn at 0.93 MeV, with ^{17}O in its ground state, and the transitions to the low lying $\frac{3}{2}^+$, $\frac{11}{2}^-$, and $\frac{1}{2}^+$ states in ^{121}Sn, with ^{17}O in its first excited $\frac{1}{2}^+$ state. In the DWBA calculations the cross sections for these transitions were added weighted by their corresponding spectroscopic factors (see Table IV).

A comparison between the experimental data and the DWBA calculations reveals several features: (1) For both cases the maximum of the angular distribution for the DWBA prediction is shifted towards larger angles by about 5°. This effect is known from other one particle transfer reactions[49] and has also been observed in the ^{54}Fe(^{18}O, ^{17}O)^{55}Fe reaction investigated at 50 MeV incident energy.[50] (2) The absolute experimental cross section, however, differs between the reactions ^{54}Fe(^{18}O, ^{17}O,)^{55}Fe and ^{120}Sn(^{18}O, ^{17}O)^{121}Sn. If we consider the fact that 3 unresolved states contribute to the data shown in Fig. 10 for ^{121}Sn, the difference in the ground state cross sections between both reactions is approximately an order of magnitude and appears to be even larger at the most forward angles. A similar difference is apparent from the data for the excited states in ^{55}Fe and ^{121}Sn. In addition, it is to be expected that more states in ^{55}Fe are populated with appreciable cross sections than in ^{121}Sn, due to the positive ground state Q value for the ^{54}Fe(^{18}O, ^{17}O)^{55}Fe reaction.

It is well known that coupled channels effects have the strongest influence on the angular distribution at forward angles.[51] This behavior, together with the fact that the cross section for one neutron transfer is much larger for ^{54}Fe than for the ^{120}Sn, suggests that the large shift $\Delta\theta$ observed in the inelastic scattering angular dis-

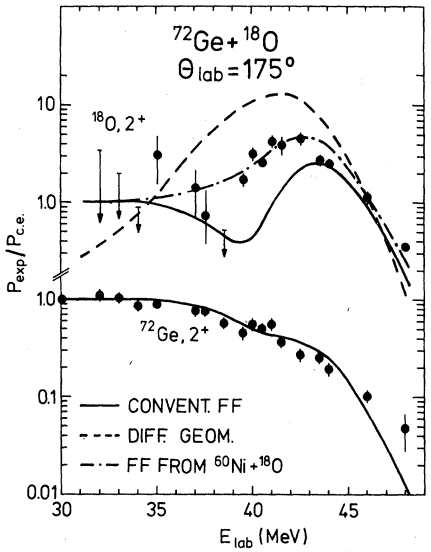

FIG. 9. Excitation functions for the system ^{18}O+^{72}Ge measured at θ_{lab}=175°. The curves are DWBA calculations as discussed in the text.

tribution of ^{18}O on ^{54}Fe is connected with coupled reaction channels effects.

So far only the one neutron transfer reaction (^{18}O, ^{17}O) has been considered as an intermediate step in CRC calculations.[16] In addition, our data

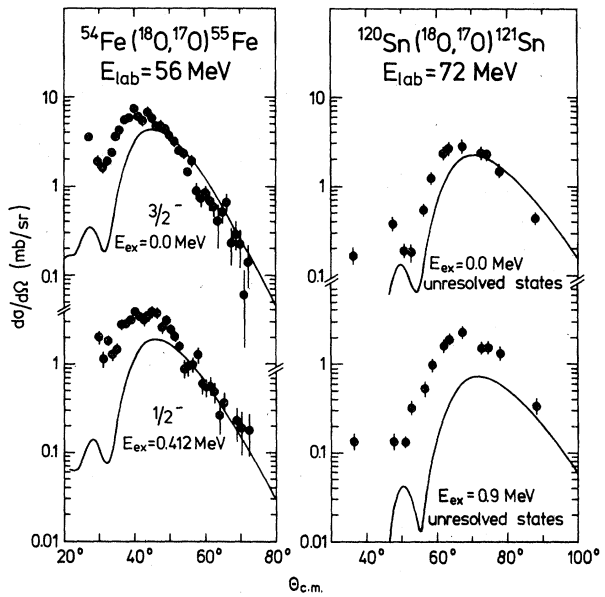

FIG. 10. One neutron transfer reactions (^{18}O, ^{17}O) for the systems ^{18}O+^{54}Fe and ^{18}O+^{120}Sn. The solid lines are DWBA calculations with parameters from Table IV.

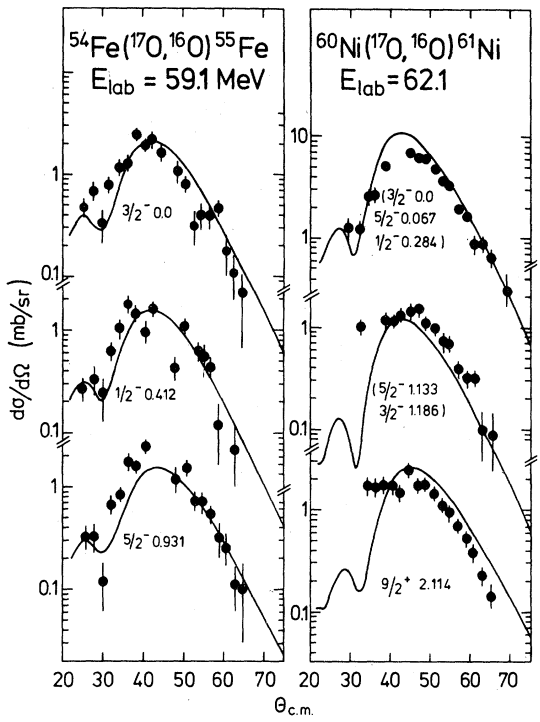

FIG. 11. One neutron transfer reactions (^{17}O, ^{16}O) for the systems ^{17}O+^{54}Fe and ^{17}O+^{60}Ni. The solid lines are DWBA calculations with parameters from Table IV.

indicate that the two neutron transfer route (^{18}O, ^{16}O)⊗[^{16}O, ^{18}O(2$^+$)] has to be taken into account. The total two neutron transfer cross section usually has the same order of magnitude as the one neutron transfer cross section. Furthermore,

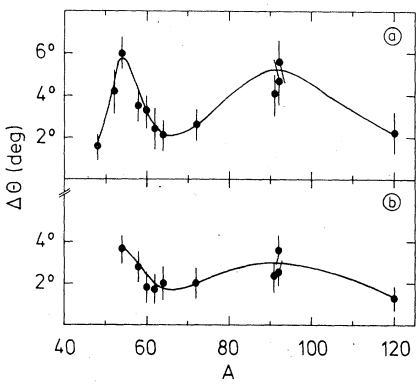

FIG. 12. (a) Angular shift $\Delta\theta$ of the last minimum in the experimental angular distribution for the excitation of ^{18}O(2$^+$) if compared to the DWBA prediction for reactions with target nuclei of mass A. (b) Same as (a) but for the preceding maximum in the angular distribution. The solid lines serve to guide the eye.

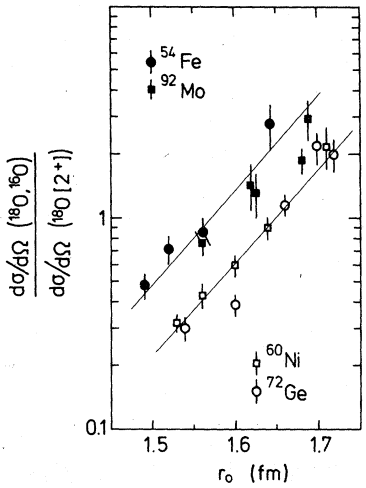

FIG. 13. Cross section ratio between the two neutron transfer reaction (^{18}O, ^{16}O) and the inelastic transition to the 2^+ state in ^{18}O as obtained from excitation functions for the systems $^{18}O+^{54}Fe$, ^{60}Ni, ^{72}Ge, ^{92}Mo measured at $\theta_{lab}=175°$. The abscissa is the normalized radius parameter as discussed in the text. The solid lines serve to guide the eye.

the (^{16}O, ^{18}O) reaction, leaving ^{18}O in its first excited state, is known to have a large cross section.[18] In order to investigate a possible correlation between the magnitude of the two neutron transfer cross section and the observed shift $\Delta\theta$ in the angular distribution for inelastic scattering of ^{18}O (2^+), we have determined the cross section ratio between the (^{18}O, ^{16}O) transfer reaction and the excitation of the 2^+ state in ^{18}O by measuring excitation functions at $\theta_{lab}=175°$ for the targets ^{54}Fe, ^{60}Ni, ^{72}Ge, and ^{92}Mo. A particle-gamma coincidence technique was employed. Experimental details are given in Ref. 5. If we assume that the states produced in the (^{18}O, ^{16}O) reaction dominantly decay via the lowest $2^+\rightarrow 0^+$ transition, this γ-gamma intensity should be proportional to the total cross section. No significant amount of feeding of the 2^+ state in ^{18}O from higher lying states was observed.

Figure 13 shows the ratio of the γ intensities between the respective $2^+\rightarrow 0^+$ transitions in the final nuclei produced in the (^{18}O, ^{16}O) reaction and the one for the $2^+\rightarrow 0^+$, 1.982 MeV transition in ^{18}O. The values are plotted as a function of a normalized radius parameter r_0 calculated from the relation

$$r_0(A_1^{1/3}+A_2^{1/3})=\frac{Z_1Z_2e^2}{2E_{c.m.}}\left[1+\csc\left(\frac{\theta}{2}\right)\right].$$

From Fig. 13 we observe that the cross section ratio is higher for the targets ^{54}Fe and ^{92}Mo than for ^{60}Ni and ^{72}Ge, indicating that the two neutron transfer cross section is larger for nuclei which show the largest shift $\Delta\theta$ in the inelastic scattering angular distributions.

Altogether, these results suggest that the shift $\Delta\theta$ between the experimental angular distributions and their DWBA predictions might be caused by one and two neutron transfer reactions contributing as intermediate steps to the excitation of ^{18}O (2^+). The influence of the static quadrupole moment, which can explain the angular distributions from Ref. 10, is too small for the case of ^{18}O as shown in Ref. 12.

D. The excitation of ^{17}O ($1/2^+$) and single neutron transfer reactions (^{17}O, ^{16}O) on ^{54}Fe and ^{60}Ni

The $\frac{5}{2}^+\rightarrow\frac{1}{2}^+$ transition in ^{17}O represents a good case for the investigation of coupled channels effects in inelastic excitation for the following reasons: (1) The $B(E2)$ value is much smaller than in the neighboring nucleus ^{18}O. Therefore, the maximum cross section in the inelastic excitation is smaller for the scattering of ^{17}O if compared to ^{18}O. Thus, intermediate routes such as the (^{17}O, ^{16}O)$\otimes$(^{16}O, $^{17}O^*$) reaction might be of influence to the angular distribution. (2) Microscopic form factor calculations can be performed for the $\frac{5}{2}^+\rightarrow\frac{1}{2}^+$ single particle transition.

The inelastic excitation of ^{17}O has been investigated with the (p,p') reaction,[52] and in connection with coherent transfer phenomena.[53,54] Owing to the low excitation energy (0.871 MeV) of the $\frac{1}{2}^+$ state in ^{17}O, the inelastic transition could only be separated from the elastic peak for angles larger than 20°. The angular distributions obtained for the elastic and inelastic scattering of $^{17}O+^{54}Fe$ and $^{17}O+^{60}Ni$ are shown in Figs. 7 and 8. The bombarding energy was chosen to correspond to the same c.m. energy used in the $^{18}O+^{54}Fe$ (this work) and $^{18}O+^{60}Ni$ (Ref. 5) studies. The solid lines in Figs. 7 and 8 represent the DWBA calculations performed with a macroscopic form factor. Since for a single particle state the nuclear deformation length δ_N cannot be calculated from the $B(E2)$ value, it was treated as a free parameter. The DWBA calculations for the excitation of the $\frac{1}{2}^+$ state in ^{17}O are in reasonable agreement with the data, in contrast to the excitation of ^{18}O (2^+) discussed previously.

The results for the one neutron transfer reactions $^{54}Fe(^{17}O, ^{16}O)^{55}Fe$ and $^{60}Ni(^{17}O, ^{16}O)^{61}Ni$ are shown in Fig. 11. The solid lines are DWBA calculations as described in Sec. III with spectroscopic factors given in Table IV. The agreement between the calculated and measured differential cross section is good, both in absolute magnitude

and in the position of the maximum.

We conclude that no obvious connection between transfer channels and inelastic scattering can be established from the present data for the systems $^{54}Fe + ^{17}O$ and $^{60}Ni + ^{17}O$; it would be necessary to obtain more accurate information on the inelastic scattering, especially at the most forward angles.

E. The excitation function for $^{72}Ge + ^{18}O$

In a recent publication[15] it has been suggested that the problems in the angular distributions for the excitation of ^{18}O (2^+) can be resolved by use of a microscopic form factor with a larger width than the usual collective form factor. This procedure, however, fails to describe the excitation functions measured at backward angles, as already shown in Ref. 5. Figure 9 presents the excitation functions for the inelastic transitions to the 2^+ states in ^{72}Ge and ^{18}O together with the DWBA predictions. The differential cross sections are normalized to the calculated Coulomb excitation cross section. It has been verified that the energy dependence of the particle-gamma angular correlation does not influence the data shown in Fig. 9.

Owing to the large $B(E2;\uparrow)$ value for the $0^+ \rightarrow 2^+$ transition, the excitation of ^{72}Ge (2^+) is dominated by the Coulomb form factor and does not show a noticeable Coulomb-nuclear interference minimum. The DWBA calculation describes this behavior. For the 2^+ state in ^{18}O the DWBA calculation (solid line in Fig. 9) underestimates the cross section at incident energies around 40 MeV by about a factor of 4. A form factor with an increased width, which describes the angular distribution for the ^{18}O (2^+) excitation measured at 68.6 MeV (dashed line in Fig. 9), overpredicts the cross section within the energy range between 37 and 45 MeV. The best result is obtained with an *ad hoc* form factor with parameters which fit the data shown in Ref. 5 for the $^{18}O + ^{60}Ni$ reaction (dot-dashed line in Fig. 9); the same form factor already successfully described the excitation function for the system $^{18}O + ^{92}Mo$ (see Ref. 5).

VI. SUMMARY AND CONCLUSIONS

We have investigated inelastic scattering and neutron transfer reactions on several target nuclei in the mass range $A = 48-92$. Except for the single particle transition in ^{91}Zr and the $0^+ \rightarrow 2^+$ transitions in ^{52}Cr and ^{54}Fe which have the smallest $B(E2)$ values, the angular distributions for the excitation of the first excited states in the target nuclei are well described by DWBA calculations with $B(E2)$ values as taken from the literature and equal charge and mass deformation lengths. This finding is different from the results of Hillis *et al.*,[7] who had to use coupled channels calculations for the reaction $^{12}C + Nd$ in order to describe the angular distributions for the first excited 2^+ states in the even Nd isotopes. The measured distributions for the excitation of the first excited state in ^{18}O are, however, shifted towards forward angles by $2°-5°$ with respect to the DWBA calculations. This angle shift $\Delta\theta$ depends on the target nucleus and is largest for nuclei near closed neutron shells. Reorientation effects in the 2^+ state in ^{18}O are too small to explain the measured shift $\Delta\theta$ as shown in Ref. 12. In addition, they cannot explain the variation of $\Delta\theta$ for different target nuclei.

The prescription[15] to use a microscopic form factor with a larger radial width in order to describe the angular distributions for the excitation of the 2^+ state in ^{18}O fails to reproduce the measured excitation functions at backward angles. We suggest that one and two neutron transfer reactions are responsible for the deviations observed in the inelastic scattering. This suggestion is supported by the fact that the cross sections for one and two neutron transfer are largest for target nuclei with a closed neutron shell and by the systematic deviations observed for inelastic scattering. These target nuclei also exhibit the largest anomalies in inelastic scattering.

Inelastic scattering with target and projectile excitation and one neutron transfer was also investigated with ^{17}O ions on ^{54}Fe and ^{60}Ni targets. The transfer cross sections to low lying states are well described by DWBA calculations. The present date for the inelastic scattering in the forward angular range are not accurate enough to establish definite conclusions on the influence of transfer reactions.

CRC calculations including the one neutron transfer have been performed for the system $^{18}O + ^{60}Ni$ (Ref. 16). Similar calculations including the one and two neutron transfer channels as intermediate steps should be performed in order to describe the systematic behavior observed in this investigation.

We would like to thank Dr. P. Maier-Komor, Katharina Nacke, and E. Kellner for the preparation of the targets. This work was supported by the Bundesministerium für Forschung und Technologie, Bonn.

*Present address: GSI, Darmstadt, West Germany.
[1]F. Videbaek, I. Chernov, P. R. Christensen, and E. E. Gross, Phys. Rev. Lett. 28, 1072 (1972); P. R. Christensen, I. Chernov, E. E. Gross, R. Stokstad, and F. Videbaek, Nucl. Phys. A207, 433 (1973).
[2]F. D. Becchetti, D. G. Kovar, B. G. Harvey, J. Mahoney, B. Mayer, and F. G. Pühlhofer, Phys. Rev. C 6, 2215 (1972).
[3]J. L. C. Ford, Jr., K. S. Toth, D. C. Hensley, R. M. Gaedke, P. J. Riley, and S. T. Thornton, Phys. Rev. C 8, 1912 (1973).
[4]E. E. Gross, H. G. Bingham, M. L. Halbert, D. C. Hensely, and M. J. Saltmarsh, Phys. Rev. C 10, 45 (1974).
[5]K. E. Rehm, H. J. Körner, M. Richter, H. P. Rother, J. P. Schiffer, and H. Spieler, Phys. Rev. C 12, 1945 (1975).
[6]G. R. Satchler, J. L. C. Ford, Jr., K. S. Toth, D. C. Hensley, E. E. Gross, D. E. Gustafson, and S. T. Thornton, Phys. Lett. 60B, 43 (1975).
[7]D. L.Hillis, E. E. Gross, D. C. Hensley, L. D. Rickertsen, C. R. Bingham, A. Scott, and F. T. Baker, Phys. Rev. Lett. 36, 304 (1976); D. L. Hillis, E. E. Gross, D. C. Hensley, C. R. Bingham, F. T. Baker, and A. Scott, Phys. Rev. C 16, 1467 (1977).
[8]J. Carter, R. G. Clarkson, V. Hnizdo, R. J. Keddy, D. W. Mingay, F. Osterfeld, and J. P. F. Sellschop, Nucl. Phys. A273, 523 (1976); J. Carter, R. G. Clarkson, V. Hnizdo, and J. P. F. Sellschop, *ibid.* A297, 520 (1978).
[9]Nguyen Van Sen, G. Ratel, R. Darves-Blanc, J. C. Gondrand, and F. Merchez, Phys. Rev. C 17, 639 (1978).
[10]E. E. Gross, T. P. Cleary, J. L. C. Ford, D. C. Hensley, and K. S. Toth, Phys. Rev. C 17, 1665 (1978).
[11]W. E. Frahn and K. E. Rehm, Phys. Rep. 37C, 1 (1978), and references cited therein.
[12]F. Videbaek, P. R. Christensen, O. Hansen, and K. Ulbak, Nucl. Phys. A256, 301 (1976).
[13]R. A. Broglia, in *Proceedings of the International Conference on Reactions between Complex Nuclei, Nashville, Tennessee, 1974*, edited by R. L. Robinson, F. K. McGowan, J. B. Ball, and J. H. Hamilton (North-Holland, Amsterdam, 1974), Vol. II, pp. 303–326.
[14]J. L. Artz, D. Dehnhard, D. J. Weber, R. J. Falkenberg, T. K. Li, and S. Kubono, Bull. Am. Phys. Soc. 21, 965 (1976); M. P. Fewell, D. C. Kean, R. H. Spear, and A. M. Baxter, J. Phys. G3, L27 (1977); C. Flaum, J. Barrette, M. J. LeVine, and C. E. Thorn, Phys. Rev. Lett. 39, 446 (1977); P. B. Vold, D. Cline, P. Russo, J. K. Sprinkle, R. P. Scharenberg, and R. J. Mitchell, *ibid.* 39, 325 (1977).
[15]A. J. Baltz and S. Kahana, Phys. Rev. C 17, 555 (1978).
[16]K. S. Low, in *Proceedings of the International Conference on Nuclear Structure, Tokyo, 1977*, edited by T. Marumori (Physical Society of Japan, Tokyo, 1978) [J. Phys. Soc. Jpn. Suppl. 44, 267 (1978)].
[17]N. K. Glendenning and G. Wolschin, Nucl. Phys. A281, 486 (1977).
[18]H. Spieler, H. J. Körner, K. E. Rehm, M. Richter, and H. P. Rother, Z. Phys. A278, 241 (1976).
[19]E. H. Auerbach, Brookhaven National Laboratory Report No. BNL 6532, 1962 (unpublished), modified by S. A. Zawadski, Argonne National Laboratory.
[20]We are indebted to F. Videbaek of the NBI for supplying us with the modified version of DWUCK.
[21]D. H. Gloeckner, M. H. Macfarlane, and S. C. Pieper, Argonne National Laboratory Report No. ANL-76-11, 1978 (unpublished).
[22]R. M. DeVries, G. R. Satchler, and J. G. Cramer, Phys. Rev. Lett. 32, 1377 (1974).
[23]W. Henning, Y. Eisen, J. R. Erskine, D. G. Kovar, and B. Zeidman, Phys. Rev. C 15, 292 (1977).
[24]G. M. Temmer and N. P. Heydenburg, Phys. Rev. 104, 967 (1956).
[25]P. D. Kunz (unpublished); ORNL version.
[26]A. Christy and O. Häusser, Nucl. Data Tables A11, 281 (1972).
[27]J. Bellicard and P. Barreau, Nucl. Phys. 36, 476 (1962).
[28]J. Haberkant, thesis, Heidelberg, 1973 (unpublished).
[29]L. N. Galperin, A. Z. Il'yasov, I. Kh. Lemberg, and G. A. Firsonov, Yad. Fiz. 9, 225 (1969) [Sov. J. Nucl. Phys. 9, 133 (1969)].
[30]H. F. Lutz, W. Bartolini, T. H. Curtis, and G. M. Klody, Phys. Rev. 187, 1479 (1969).
[31]B. M. Preedom, C. R. Gruhn, T. Y. T. Kuo, and C. J. Maggiore, Phys. Rev. C 2, 166 (1970).
[32]G. S. Mani, Nucl. Phys. A157, 471 (1970).
[33]C. M. Perey, R. J. Silva, J. K. Dickens, and F. G. Perey, Phys. Rev. C 2, 468 (1970).
[34]T. H. Curtis, H. F. Lutz, and W. Bartolini, Phys. Rev. C 1, 1418 (1970).
[35]Y. Awaya, K. Matsuda, N. Nakanishi, S. Takeda, and T. Wada, J. Phys. Soc. Jpn. 27, 1087 (1969).
[36]M. M. Stautberg and J. J. Kraushaar, Phys. Rev. 151, 969 (1966).
[37]O. Hansen, T. A. Belote, and W. E. Dorenbusch, Nucl. Phys. A118, 41 (1968).
[38]F. T. Baker, S. Davis, C. Glashausser, and A. B. Robbins, Nucl. Phys. A233, 409 (1974).
[39]R. K. Jolly, Phys. Rev. 139, B318 (1965).
[40]E. R. Flynn, D. D. Armstrong, and G. J. Beery, Phys. Rev. C 1, 703 (1970).
[41]H. P. Morsch and R. Santo, Phys. Lett. 37B, 491 (1971).
[42]D. E. Rundquist, M. K. Brussel, and A. I. Yavin, Phys. Rev. 168, 1287 (1968).
[43]A. M. Bernstein, E. P. Lippincott, G. T. Sample, and C. B. Thorn, Nucl. Phys. A115, 79 (1968).
[44]G. Bruge, J. C. Faivre, H. Faraggi, and A. Bussiere, Nucl. Phys. A146, 597 (1970).
[45]A. A. Cowley, P. M. Cronje, G. Heymann, S. J. Mills, and J. C. Van Staden, Nucl. Phys. A229, 256 (1974).
[46]C. R. Bingham, M. L. Halbert, and A. R. Quinton, Phys. Rev. 180, 1197 (1969).
[47]P. J. Moffa, C. B. Dover, and J. P. Vary, Phys. Rev. C 13, 147 (1976).
[48]F. D. Becchetti, P. R. Christensen, V. I. Manko, and R. J. Nickles, Nucl. Phys. A203, 1 (1973).
[49]R. H. Siemssen, C. L. Fink, L. R. Greenwood, and H. J. Körner, Phys. Rev. Lett. 28, 626 (1972).
[50]J. F. Petersen, D. Dehnhard, and B. F. Bayman, Phys. Rev. C 15, 1719 (1977).
[51]N. K. Glendenning and G. Wolschin, Phys. Rev. Lett. 34, 1642 (1975).
[52]G. B. Crinean, L. W. J. Wild, and B. M. Spicer, Nucl. Phys. A244, 67 (1975).
[53]C. K. Gelbke, G. Baur, R. Bock, P. Braun-Munzinger, W. Grochulski, H. L. Harney, and R. Stock, Nucl. Phys. A219, 253 (1974); D. Kalinsky, D. Melnik, U. Smilansky, N. Trautner, B. A. Watson, Y. Horowitz, S. Mordechai, G. Baur, and D. Pelte, *ibid.* A250, 364 (1975).
[54]R. Chechik, Z. Fraenkel, H. Stocker, and Y. Eyal, Nucl. Phys. A287, 353 (1977).

[55]J. R. Maxwell and W. C. Parkinson, Phys. Rev. 135, B82 (1964).
[56]M. Pignanelli, J. Gosset, F. Resmini, B. Mayer, and J. L. Escudié, Phys. Rev. C 8, 2120 (1973).
[57]E. J. Schneid, A. Prakash, and B. L. Cohen, Phys. Rev. 156, 1316 (1967).
[58]R. Mendelson, J. C. Hardy, and J. Cerny, Phys. Lett. 31B, 126 (1970).
[59]J. Vervier, Nucl. Data B2, 5–81 (1968).